CHINESE OPTICS LETTERS

Vol. 22, No. 5 | May 2024

MLSE-assisted decision feedback equalizer for error-propagation suppression in high-speed IM-DD transmission systems

Jiahao Zhou (周家豪)[1], Jing Zhang (张 静)[1*], Xue Zhao (赵 雪)[1], Rui Wang (王 芮)[1], Jinjiang Li (李劲江)[1], Shaohua Hu (胡少华)[1], Qianwu Zhang (张倩武)[2], Qi Yang (杨 奇)[3], Bo Xu (许 渤)[1], and Kun Qiu (邱 昆)[1]

[1] Key Laboratory of Optical Fiber Sensing and Communication, University of Electronic Science and Technology of China, Chengdu 611731, China

[2] Key Laboratory of Specialty Fiber Optics and Optical Access Networks, Shanghai University, Shanghai 200444, China

[3] School of Optical and Electronic Information, Huazhong University of Science and Technology, Wuhan 430074, China

*Corresponding author: zhangjing1983@uestc.edu.cn

Received January 15, 2024 | Accepted February 5, 2024 | Posted Online May 17, 2024

We propose a trellis-compressed maximum likelihood sequence estimation (TC-MLSE)-assisted sliding-block decision feedback equalizer (DFE) to suppress the error propagation resulting from the DFE in high-speed systems. We use an out-of-range detector to detect the end of burst errors from the DFE and activate the optional TC-MLSE to correct burst errors. We conduct experiments to transmit a 201-Gbit/s PAM-8 signal. The results show that the proposed method achieves a bit error rate of 3.65×10^{-3}, which is close to that of MLSE. The optional MLSE is only activated when needed and processes 11.4% of the total symbols. Moreover, the proposed method compresses the maximum length of burst errors from 19 to 5.

Keywords: intensity modulation; direct detection; sliding-block decision feedback equalizer; error propagation; maximum likelihood sequence estimation; out-of-range detector.

DOI: 10.3788/COL202422.050604

1. Introduction

Driven by various emerging internet services, there is an exponentially increasing requirement of the data traffic in data center interconnects (DCIs). In recent years, the data traffic of intra-DCIs (East–West traffic) is significantly greater than that of inter-DCIs (North–South traffic)[1]. Intra-DCIs that cover 2-km transmission distance are very sensitive to the cost and power consumption. Intensity modulation and direct-detection (IM-DD), employing M-level pulse amplitude modulation (PAM), is preferred as a cost-effective solution due to its low power consumption and simple transceiver design. For next-generation 800-Gb or 1.6-Tb Ethernet links larger than 200 Gb/s per lane are expected to reduce the complexity of integration[2,3]. With the increasing data rate in short-reach applications, the compensation of large inter-symbol interference (ISI) caused by severe bandwidth limitation and chromatic dispersion has become extremely challenging[4].

An adaptive channel-matched detection (ACMD) that includes a polynomial nonlinear equalizer, a decision feedback equalizer (DFE), and maximum likelihood sequence estimation (MLSE) has been investigated to effectively compensate most of the link distortion based on the noise characteristics[5]. The DFE is usually combined with a feed forward equalizer (FFE) to deal with post-cursor and post-cursor ISI simultaneously. However, the error propagation in the DFE degrades the transmission performance and reduces the coding gain offered by popular forward error correction (FEC) codes[6,7]. An erasure DFE that feeds back the boundary of possible symbols when the equalized symbol is recognized as an "unreliable symbol" has been studied to suppress error propagation[8,9]. However, the erasure DFE cannot completely break long burst errors. Employing differential precoding can break burst errors resulting from DFE. But this needs to alter the transmitter-side digital signal processing (DSP). Additionally, a single random error turns into two errors after the precoding is removed. Therefore, the transmission performance is degraded in scenarios where the correlation of errors is less severe[10].

A weighted DFE (WDFE) that introduces the reliability to control the weight of feedback symbol has been studied to suppress the burst error propagation[11]. However, a large-memory-length MLSE is needed after the WDFE to compensate the residual ISI. Additionally, different variations of the WDFE have been investigated to suppress the error propagation from the DFE for high-rate transmission systems[12]. Moreover, a state-tracking DFE that recursively infers the probability of the biased

state is investigated to suppress the error propagation of the DFE[13], whereas the recursive operation severely hinders its evolution to multi-tap the DFE. On the other hand, it is challenging to realize a pipelined and high-speed DFE due to the feedback timing constrains. Loop-unrolling architecture is a well-known method used to relax the timing constraints[14]. However, the area and power consumption of this method increase exponentially with the tap count in the DFE, still limiting the data rate of the DFE. A sliding-block (SB)-DFE that partitions the signal into overlapping but computationally independent blocks has been investigated to break the feedback loop and achieve high-speed DFE[15], while the SB-DFE omits the issue of error propagation. Moreover, the MLSE that considers the pattern-dependent ISI between the adjacent symbols outperforms the DFE but with a larger computational complexity. A trellis-compressed MLSE (TC-MLSE) has been investigated in our previous work[16], which greatly reduces the implementation complexity. Even so, the TC-MLSE is more power hungry than the DFE. Thus, it is highly desirable to investigate a low-power-consumption pathway to suppress the error propagation resulting from the DFE in high-speed IM-DD systems.

In this Letter, we propose and experimentally demonstrate a TC-MLSE-assisted SB-DFE with lower power consumption to suppress the burst errors resulting from the DFE. The SB-DFE divides the received signal into blocks, with each block overlapping with its neighbors by several symbols. Thus, the SB-DFE can be pipelined. The burst errors of the DFE terminate when the equalized signal is out of range. We employ an out-of-range (OOR) detector after the DFE to monitor the OOR symbol for each block. This can identify the consecutive error block resulting from the DFE. Due to different error mechanisms of the MLSE and the DFE, the consecutive errors can be suppressed by the MLSE. Therefore, an optional TC-MLSE can be activated to correct the errors. Once a signal exceeds the OOR threshold, the TC-MLSE can be activated to mitigate the error propagation. We compare the proposed TC-MLSE-assisted SB-DFE with a traditional DFE and an individual TC-MLSE in a 67-Gbaud PAM-8 signal transmission over a 2-km standard single-mode fiber (SSMF) IM-DD system at the C-band. The experimental results show that the TC-MLSE-assisted SB-DFE achieves a similar performance to that of the MLSE for the 67-Gbaud PAM-8 signal transmission but with lower power consumption. Moreover, the maximum length of burst consecutive errors of the DFE is reduced from 19 to only 5. This results in a 0.1 normalized generalized mutual information (NGMI) improvement compared to the SB-DFE.

2. Principle

Figure 1 shows the schematic of the TC-MLSE-assisted SB-DFE. In the SB-DFE, the received signal is divided into blocks and processed in parallel. Each block consists of an 'overlap part' and a 'decode part' with a fixed length. The DFE loop is only performed within one block. For each block, the overlap part is used to seed the decoding part by using the hard decision

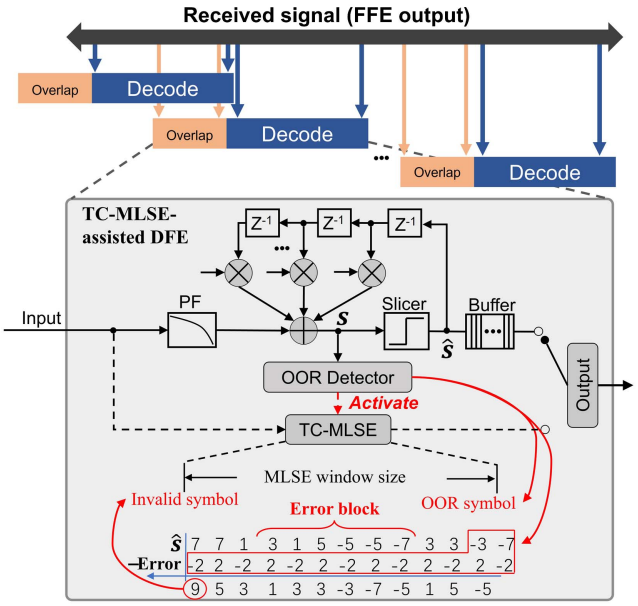

Fig. 1. Block diagram of the TC-MLSE-assisted SB-DFE.

resulting from the FFE output, which does not depend on the decision of the previous block. This breaks the feedback loop in the traditional DFE. Because the data flow through the SB-DFE is exclusively feedforward, it can be pipelined to meet the challenges of latency requirements. The reliability of the decisions in the SB-DFE improves along the block and converges with the traditional DFE with the same taps. Eventually, the overlap part is discarded and only the decoding part is reserved as the output. Note that the length of the overlap part can be set to two, which is larger than the tap number of the DFE, to avoid performance penalty. For the PAM signal, the burst errors resulting from the DFE exhibit '+2, −2' zig-zag pattern[17]. Specially, when the true symbol is already at the top level, one level higher than this level makes no difference after the decision, so the error propagation is terminated. Additionally, the equalized symbol of the DFE exceeds the standard top level, and we regard it as an OOR symbol. Similarly, if the true symbol is already at the floor level, one level lower than it does not change the decision result, and the equalized symbol of DFE is lower than the floor level. The error propagation terminates in two such particular cases. So we can find out the consecutive errors by monitoring the OOR symbols. On the other hand, we have studied the burst consecutive errors resulting from the MLSE in our previous work[18]. Several consecutive symbols that have large noise of the same polarity leads to the mismatch between the estimated path and the true path, finally resulting in consecutive errors in the MLSE. While an incorrect decision on a certain symbol leads to the error propagation in the DFE, different mechanisms of error propagation between the DFE and the MLSE result in different error distributions. Therefore, we can use an optional MLSE to correct the burst errors resulting from the DFE, i.e., the proposed TC-MLSE-assisted DFE. This optional TC-MLSE is only activated when the OOR identifies the error block of the DFE.

In the TC-MLSE-assisted DFE, the $(N+1)$-tap post filter (PF) is employed to suppress the noise enhancement caused by the FFE, and the N-tap DFE cancels the trailing ISI resulting from the PF. We employ an OOR detector in the DFE loop to supervise whether the DFE's output is an OOR symbol. If the equalized signal of the DFE does not exceed the preset OOR threshold, then the DFE provides the output sequence, while the TC-MLSE is inactive. Once a symbol exceeds the OOR threshold, it indicates that the preceding sequence may suffer from error propagation, and the current symbol is the end of the burst errors. Immediately, the optional TC-MLSE is activated to search the most likely transmitted sequence, corresponding to the sequence suffering from error propagation. To ensure that the MLSE works stably, the MLSE window must contain the beginning of the error propagation.

In this work, we find that the beginning of the error block can be found by subtracting the estimated errors from the estimated symbols $\hat{\mathbf{s}}$, as shown in the 'MLSE window size' module of Fig. 1. Clearly, the sign of the estimated error at the end of error block is the same as the OOR symbol. For instance, if the OOR symbol is lower than -3, the corresponding estimated error is -2. Thus, we can easily infer the error propagation values 'Error' for previous symbols by the regulation that the error propagation alternates in the '$+2$, -2' pattern. Then, we subtract the estimated errors from $\hat{\mathbf{s}}$. For symbols in the consecutive error block, this recovers expected symbols, while this may produce an invalid symbol for the symbols outside the error block, i.e., 9 (for the PAM-8 signal) in this example. Therefore, we set the MLSE window to start at this invalid symbol and finish at the OOR symbol, containing the beginning of the error propagation. Note that if we cannot find such an invalid symbol within the data block, we set the MLSE window to start at the beginning of the data block. During the period of error propagation, the TC-MLSE module provides the output. After the error propagation terminates, the output switches back to the DFE. The processing delay of the DFE differs from the MLSE, so a buffer is needed after the DFE output to make this switch seamless.

Moreover, the performance of the TC-MLSE-assisted DFE is related to the preset OOR threshold. If it is too large, then we may miss the true error propagation blocks, resulting in a performance close to DFE-based receiver, while too small OOR threshold will be triggered by noise instead of burst error. This makes no improvement for the equalizer performance but only leads to unnecessary power consumption. Therefore, we should choose the largest OOR threshold among the thresholds that meet the performance requirement. For this issue, we simulate the relationship between the OOR threshold and the performance of the TC-MLSE-assisted DFE. Figure 2 depicts the probability of successfully detecting error propagations versus different OOR thresholds in a $1+\alpha D$ channel with a PAM-8 signal. The horizontal axis of Fig. 2 represents the gap between the OOR threshold and the top level, i.e., $+7$ for the PAM-8 signal. In Fig. 2, for each α, the optimal OOR threshold is located around the point whose gap with the top level is equal to α, as shown with the red stars. In addition, we summarize the required number of multiplications of different equalization schemes in Table 1. The TC-MLSE reserves the P probability for each symbol to reduce the complexity[16]. Although activating the TC-MLSE increases the complexity, the TC-MLSE in the proposed scheme is only activated when the error propagation of the DFE is detected.

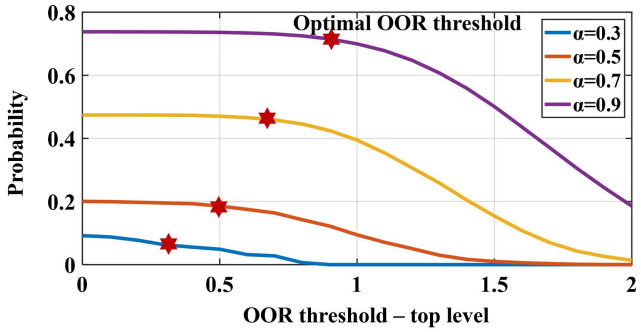

Fig. 2. Probability of successfully detecting the error propagation versus the OOR threshold in a $1+\alpha D$ channel with a PAM-8 signal.

Table 1. Complexity Comparison of Different Equalizers.

Equalizers	Multiplication Number
K-tap FFE + $(N+1)$-tap PF + N-tap DFE	$K+2\times N$
K-tap FFE + $(L+1)$-tap PF + TC-MLSE	$K+P^{(L+1)}+L$
TC-MLSE-assisted DFE	$K+P^{(L+1)}+2\times N+L$

3. Experimental Setup

Figure 3 shows the experimental setup of the PAM signal IM-DD transmission system at the C-band. At the transmitter, a $(2^{20}-1)$-points pseudo-random bit sequence (PRBS) has been used to generate the digital PAM-8 signal off-line and then is shaped by a root raised cosine (RRC) filter with a 0.05 roll-off factor. Then, the 67-Gbaud PAM-8 signal with a 35.175-GHz

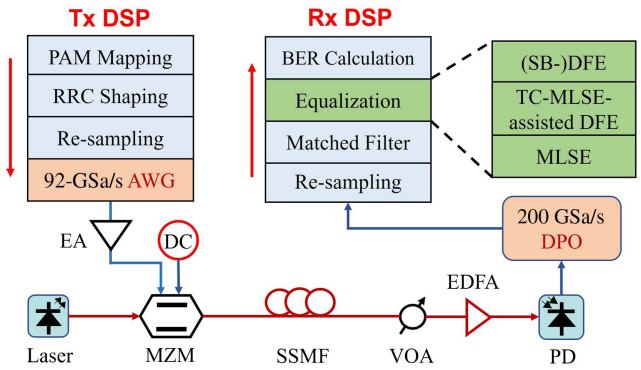

Fig. 3. Experimental setup of the IM-DD system.

bandwidth is generated via fractional sampling with the 32-GHz bandwidth arbitrary waveform generator (AWG) operating at 92 GSa/s. After being amplified by an electrical amplifier (EA), a single-drive mode Mach–Zehnder modulator (MZM) with 40 GHz is used for electro/optic conversion. A 1.89-V DC bias is applied on the MZM. Then, a continuous-wave optical carrier at 1549.5 nm with 12.9-dBm optical power is launched into the MZM, and the output power of the MZM is 3.9 dBm. Next, the generated optical PAM-8 signal is fed into the 2-km SSMF with a 0.2-dB/km fiber loss. At the receiver side, a variable optical attenuator (VOA) is employed to adjust the received optical power (ROP). Given that our receiver employs a photodiode (PD) without a trans-impedance amplifier (TIA), we apply an erbium-doped fiber amplifier (EDFA) to boost the optical signal. Then, the optical signal is directly detected via a TIA-free single-ended PD with 3-dB bandwidth of 59 GHz and captured by a digital phosphor oscilloscope (DPO) operating at 200 GSa/s. Subsequently, the received signal is processed by offline DSPs, including resampling, matched filter, equalization, decoding, PAM de-mapping, and BER calculation. For equalizations, we employ and compare the proposed TC-MLSE-assisted SB-DFE with the traditional DFE, the SB-DFE, and the individual TC-MLSE.

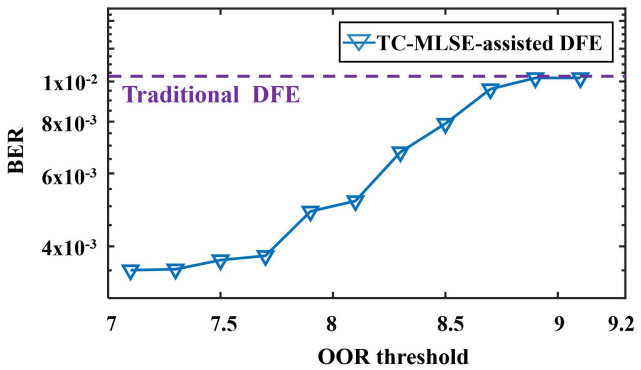

Fig. 4. BER performance of the TC-MLSE-assisted DFE versus the OOR threshold for the 67-Gbaud PAM-8 signal transmission at an ROP of 10 dBm.

4. Results and Discussion

Since the performance of the TC-MLSE-assisted DFE and power consumption rely on the OOR threshold, we first optimize the OOR threshold in the TC-MLSE-assisted DFE. Figure 4 shows the BER performance of the TC-MLSE-assisted DFE versus the OOR threshold for 67-Gbaud PAM-8 signal transmission. We also employ a traditional DFE with a first tap weight of 0.76 for comparison. In Fig. 4, the performance of the TC-MLSE-assisted DFE eventually gets close to that of the traditional DFE when the OOR threshold is increased up to 8.9. This is because a mass of endpoints of burst are missed. In addition, the performance tends to be floor level when the threshold is less than 7.7. The gap between the optimal OOR threshold and the top level (7.7–7) is close to the estimated channel response weight (0.76). This result is consistent with the previous analysis.

We then evaluate the performance of the TC-MLSE-assisted DFE to suppress the burst consecutive errors from the DFE in the 67-Gbaud PAM-8 signal transmission over the 2-km SSMF system. For comparison, we employ a traditional DFE (85, 4), an SB-DFE (85, 4), a TC-MLSE-assisted SB-DFE (85, 4), and a TC-MLSE with the memory length $L = 2$ for equalization. Because the SB-DFE is not the focus of this work, we set the size of the overlap part and the decoding part to 6 and 40 according to the rules in Ref. [15]. Figure 5(a) presents the BER performance of different equalizers. In Fig. 5(a), the SB-DFE provides a similar performance to the traditional FFE-DFE, which fails to reach the 7% overhead hard-decision FEC (HD-FEC) limitation. However, the TC-MLSE-assisted SB-DFE achieves a BER of 3.65×10^{-3} at an ROP of 10 dBm. Additionally, the overall performance of the TC-MLSE-assisted SB-DFE is close to that of the individual TC-MLSE. This improvement is because the auxiliary TC-MLSE suppresses the error propagation and is only activated when needed, and it can save power consumption compared with the always-working MLSE. Figure 5(b) shows the NGMI as a function of different ROPs for the SB-DFE and the TC-MLSE-assisted SB-DFE. Note that we calculate the NGMI with the approximate log-likelihood ratio (LLR)[19]. In Fig. 5(b), at a low ROP region, the NGMI performance of the TC-MLSE-assisted SB-DFE is slightly worse than that of the SB-DFE. This is because when the SNR is lower, in addition to the burst errors, the OOR detector may also be

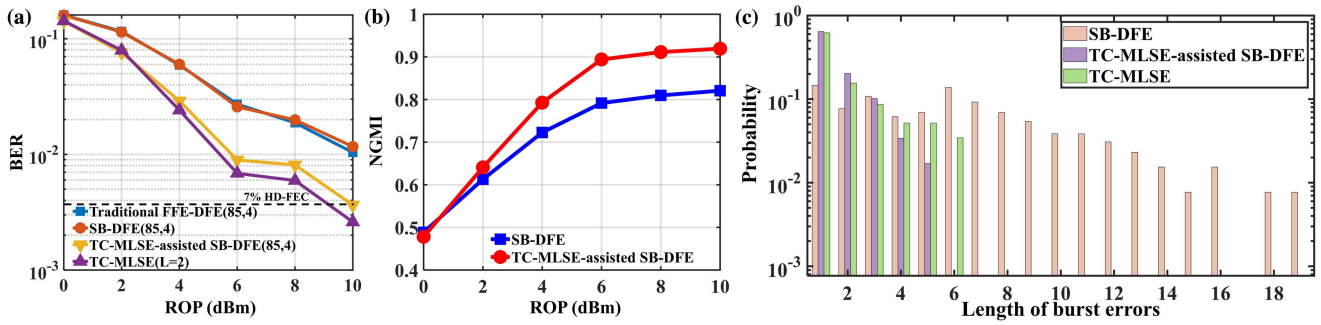

Fig. 5. (a) BER performance, (b) NGMI, and (c) burst error distribution of the 67-Gbaud PAM-8 signal transmission processed by different equalizers.

triggered by noise. At the ROP of 10 dBm, the NGMI improvement is up to 0.1 with the proposed method. The results indicate that the TC-MLSE-assisted SB-DFE can relieve the requirement and consumption of the follow-up FEC decoding. Figure 5(c) shows the burst consecutive errors distribution of the 67-Gbaud PAM-8 signal processed after the traditional DFE, the individual TC-MLSE, and the TC-MLSE-assisted SB-DFE at an ROP of 10 dBm. For the traditional DFE, the maximum length of the error block can be up to 19, which seriously degrades its performance. However, the maximum length of burst consecutive errors with the TC-MLSE-assisted SB-DFE is reduced to five. On the other hand, we count the number of bits that were processed by the MLSE for this experiment. The results show that about 11.4% of the total symbols were processed by the TC-MLSE, and the remaining bits were processed by the DFE, which indicates that the proposed TC-MLSE-assisted SB-DFE achieves a similar performance to the always-working MLSE but saves the power consumption.

5. Conclusion

In this work, we have proposed and experimentally demonstrated that the TC-MLSE-assisted SB-DFE can suppress burst consecutive errors resulting from the DFE in high-speed PAM signal transmission IM-DD systems with severe bandwidth limitations. The experimental results show that the proposed method provides a similar performance to the MLSE. Since the auxiliary TC-MLSE is only activated when detecting the end of the burst, we can save the power consumption compared with the always-working MLSE. Additionally, the maximum length of burst errors is reduced from 19 to 5 with the proposed method, which achieves 0.1 NGMI gain. We believe that the proposed TC-MLSE-assisted SB-DFE is a promising method for processing the deteriorated signals in high-speed IM-DD systems.

Acknowledgements

This work was supported by the National Natural Science Foundation of China (NSFC) (Nos. 62301128, 61871082, and 62111530150), the Open Fund of IPOC (BUPT) (No. IPOC2020A011), the STCSM (No. SKLSFO2021-01), and the Fundamental Research Funds for the Central Universities (Nos. ZYGX2020ZB043 and ZYGX2019J008).

References

1. S. J. Ben Yoo, "Optics enabled networks and architectures for data center cost and power efficiency [Invited]," J. Lightwave Technol. **40**, 2214 (2022).
2. X. Guo, X. Xue, F. Yan, *et al.*, "DACON: a reconfigurable application-centric optical network for disaggregated data center infrastructures [Invited]," J. Opt. Commun. Netw. **14**, A69 (2022).
3. S. Kanazawa, H. Yamazaki, Y. Nakanishi, *et al.*, "214-Gb/s 4-PAM operation of flip-chip interconnection EADFB laser module," J. Lightwave Technol. **35**, 418 (2017).
4. J. Zhou, H. Wang, J. Wei, *et al.*, "Adaptive moment estimation for polynomial nonlinear equalizer in PAM8-based optical interconnects," Opt. Express **27**, 32210 (2019).
5. H. Wang, J. Zhou, D. Guo, *et al.*, "Adaptive channel-matched detection for C-Band 64-Gbit/s optical OOK system over 100-km dispersion-uncompensated link," J. Lightwave Technol. **38**, 5048 (2020).
6. A. Mahadevan, Y. Lefevre, W. Lanneer, *et al.*, "Impact of DFE on soft-input LDPC decoding for 50G PON," in *Optical Fiber Communication Conference (OFC)* (2021), p. 1.
7. M. Yang, S. Shahramian, H. Shakiba, *et al.*, "Statistical BER analysis of wireline links with non-binary linear block codes subject to DFE error propagation," IEEE Trans. Circuits Syst. I: Regul. Pap. **67**, 284 (2020).
8. M. Chiani, "Introducing erasures in decision-feedback equalization to reduce error propagation," IEEE Trans. Commun. **45**, 757 (1997).
9. M. Reuter, J. C. Allen, J. R. Zeidler, *et al.*, "Mitigating error propagation effects in a decision feedback equalizer," IEEE Trans. Commun. **49**, 2028 (2001).
10. A. Mahadevan, D. Veen, N. Kaneda, *et al.*, "Hard-input FEC evaluation using Markov models for equalization-induced correlated errors in 50G PON," J. Opt. Commun. Netw. **13**, A100 (2021).
11. J. Zhou, C. Yang, D. Wang, *et al.*, "Burst-error-propagation suppression for decision-feedback equalizer in field-trial submarine fiber-optic communications," J. Lightwave Technol. **39**, 4601 (2021).
12. T. Wettlin, T. Rahman, S. Calabro, *et al.*, "Investigation of weighted DFE for high-rate short-reach transmission," in *27th Opto-Electronics and Communications Conference (OECC) and 2022 International Conference on Photonics in Switching and Computing (PSC)* (2022), p. 1.
13. K. Wu, G. Liga, J. Lee, *et al.*, "DFE state-tracking demapper for soft-input FEC in 800G data center interconnects," in *European Conference on Optical Communication (ECOC)* (2022), paper We3C.2.
14. Y. Yu, Y. Che, T. Bo, *et al.*, "Low-complexity, loop-unrolled decision-feedback equalizer for IM/DD system using PAM formats," in *Optical Fiber Communications Conference and Exhibition (OFC)* (2021), paper Th1A.44.
15. J. Bailey, H. Shakiba, E. Nir, *et al.*, "A 112-Gb/s PAM-4 low-power nine-tap sliding-block DFE in a 7-nm FinFET wireline receiver," IEEE J. Solid-State Circuits **57**, 32 (2022).
16. J. Zhou, J. Zhang, X. Zhao, *et al.*, "Simplified TC-MLSE equalizer for 210-Gb/s PAM-8 signal transmission in IM/DD systems," in *Optical Fiber Communications Conference and Exhibition (OFC)* (2022), paper M2H.4.
17. Y. C. Lu, H. Wang, D. Tonietto, *et al.*, "DFE error propagation characteristics in real 56 Gbps PAM4 high-speed links with pre-coding and impact on the FEC performance," in *Proc. DesignCon* (2017), p. 9.
18. J. Zhou, J. Zhang, X. Zhao, *et al.*, "Burst errors suppression for MLSE in high-speed IM/DD transmission systems using PAM," Opt. Express **31**, 19116 (2023).
19. A. J. Viterbi, "An intuitive justification and a simplified implementation of the MAP decoder for convolutional codes," IEEE J. Sel. Areas Commun. **16**, 260 (1998).